

# Simultaneous *uvby* photometry of the new $\delta$ Sct-type variable HD 205

E. Rodríguez<sup>1</sup>, V. Costa<sup>1</sup>, G. Handler<sup>2,3</sup>, and J. M. García<sup>4</sup>

<sup>1</sup> Instituto de Astrofísica de Andalucía, CSIC, PO Box 3004, 18080 Granada, Spain

<sup>2</sup> South African Astronomical Observatory, PO Box 9, Observatory 7935, Cape Town, South Africa

<sup>3</sup> Astronomisches Institut der Universität Wien, Türkenschanzstr. 17, 1180 Wien, Austria

<sup>4</sup> Departamento de Física, E.U.I.T. Industriales, UPM, Ronda de Valencia 3, 28012 Madrid, Spain

Received 10 July 2002 / Accepted 18 November 2002

**Abstract.** The star HD 205 has been discovered to be a new  $\delta$  Sct-type pulsator through simultaneous *uvby* photometric observations carried out during the autumn of 2001. A few  $H_\beta$ -Crawford measurements were also collected. The calibration of the Strömberg photometric indices places this star in the middle part of the  $\delta$  Sct instability strip. The behaviour of the light curves is shown to be very complex with a lot of frequencies necessary to fit the data. The data in the bands *v*, *b* and *y* were analyzed separately to confirm detected pulsations and then combined using a weighting scheme to maximize the signal-to-noise ratio. Nine frequencies were detected with the present data, but several more are probably present. The majority of the detected frequencies are due to nonradial low order p-modes as is common in  $\delta$  Sct variables.

**Key words.** stars: variables:  $\delta$  Scu – stars: individual: HD 205 – stars: oscillations – techniques: photometric

## 1. Introduction

The star HD 205 (SAO 10893,  $V = 8^m73$ , A5, Simbad 2002) was discovered as a new variable while used as one of the check stars for photometric observations of the AC And-type pulsator V823 Cas (GSC 04018-01807,  $V = 11^m4$ , main period  $P_1 = 0^d51$ ,  $\Delta V \sim 0^m5$ , Antipin 1997; Rodríguez & Breger 2001). The variability of HD 205 was obvious since the first night of observations with a main period of about 4 hours and amplitude of  $0^m05$  peak to peak, but multiperiodicity with a very complex behaviour in the light curves was also evident in the following nights. Due to the preliminary characteristics of this star (photometric indices and behaviour of the light curve) it was immediately recognized as a new  $\delta$  Sct variable and promised to be a very good target for investigation of its multiperiodicity. Thus, care was taken to observe the new variable at the same time as our main target V823 Cas. Here we present the results of this investigation for HD 205.

## 2. Observations

The observations were carried out between October and November of 2001 using the 90 cm telescope at Sierra Nevada Observatory, Spain. The photometer attached to this telescope is a six-channel spectrograph photometer (Nielsen 1983) with possibilities for simultaneous measurements in the four *uvby* filters or in two filters centered on the  $H_\beta$  line of the Strömberg-Crawford photometric system. The great majority

of the observations collected in this run were in *uvby*. A few points were obtained in  $H_\beta$  for calibration purposes.

An extended observing sequence with two variables (E1 = V823 Cas; E2 = HD 205) and two comparison stars (C1 = HD 225273,  $V = 8^m14$ , F5; C2 = HD 912,  $V = 8^m08$ , G0) was used. This sequence was possible because of the relatively long pulsational periods of V823 Cas and HD 205. The sequence was, in general, Sky, C1, E1, E2, E2, C1, C2, E1, E2. This means one point of E1 and E2 about every 5 and 3 min, respectively. When the weather conditions were not excellent, the sequence was shortened with either E2 or E2 and C2 eliminated for better monitoring of the variations of E1. As a result, HD 205 was observed in *uvby* on 13 nights, with a total of 905 points obtained during 60 hours of observation.

Each integration lasted 30 s for C1 and C2 and 40 s for HD 205. This way, an internal error per observation better than  $0^m004$  due to Poisson fluctuations is secured for each of the stars and filters. In the particular case of the *v* band, the internal error per observation was about 1.75 mmag for each of the three stars. The extinction corrections were based on nightly coefficients determined from the main comparison star. Then, magnitude differences of each object relative to C1 were calculated by means of linear interpolation. No variations were detected for C1 or C2 during the present observations, and no noticeable nightly zero-point shifts were found. In fact, the mean values obtained for the C2-C1 differences on each of the nights were always the same within  $0^m002$ , as standard deviation, for any of the filters. The standard deviations of C2-C1 were found to

Send offprint requests to: E. Rodríguez, e-mail: eloy@iaa.es

be  $0^m0077$ ,  $0^m0037$ ,  $0^m0034$  and  $0^m0041$  for  $u$ ,  $v$ ,  $b$  and  $y$  respectively, for the full data set.

To transform our instrumental magnitude differences into the standard  $uvby\beta$  system, we have used the transformation equations obtained by Rodríguez et al. (1997). The standard magnitude differences of variable minus C1 versus Heliocentric Julian Day have been deposited in the Commission 27 IAU Archives of Unpublished Observations, file 349E, and can also be requested from the authors. These derived standard differences are in excellent agreement with those we can find from the bibliography (Olsen 1983, 1996; Hauck & Mermilliod 1998). The corresponding light curves are shown in Fig. 4 where the complex behaviour of this variable can be seen.

### 3. Photometry

To derive the absolute standard Strömgren-Crawford indices for each of our stars, the  $uvby\beta$  values for C1 listed in the homogeneous catalogue of Olsen (1996) were used as zero-point. Then the corresponding values of C2 and HD 205 were calculated. Indices for C2 and HD 205 are also listed in the same catalogue. Thus the same procedure was repeated assuming these two stars as zero-point. The derived standard  $uvby\beta$  indices are listed in Table 1 together with the number of points collected for each object and the standard deviations of the magnitude differences relative to C1. The larger errors in  $V$  and  $c_1$  of HD 205 are due to the intrinsic photometric variations of this star.

As can be seen, the derived indices are in very good agreement with those listed by Olsen (1996). The same is valid when we compare with the values given in the catalogue of Hauck & Mermilliod (1998) except for a small difference in the  $V$  value of HD 205. Hauck & Mermilliod (1998) list  $V = 8^m753$  for this star as a mean between the values of  $8^m733$  from Olsen (1983; identical to Olsen 1996) and  $8^m77$  from Perry & Johnston (1982). Very probably, part of this deviation may be due to the latter authors collecting the  $V$  data during a main light minimum. This thinking is also supported by the low value of  $c_1 = 0^m891$  which these authors also list.

#### 3.1. Comparison stars

The indices given in Table 1 for each star are also in good agreement with the spectral types published in the literature (Simbad 2002). In the H-R diagram HD 205 lies inside the  $\delta$  Sct instability strip whereas C1 and C2 are outside the cool border. C1 and C2 are also not expected to be  $\gamma$  Dor-type pulsators, as shown in Fig. 1 where the observational  $\delta$  Sct and  $\gamma$  Dor regions are drawn. In the case of C1 and C2, the indices were dereddened using Crawford's (1975) calibration for F-type stars. To calculate the corresponding absolute visual magnitudes, mean values between the luminosities derived from these calibrations and those from the parallaxes determined by the Hipparcos satellite (ESA 1997) were used ( $\pi = 6.02(\pm 0.81)$  mas for C1 and  $\pi = 9.34(\pm 0.82)$  mas for C2).

**Table 1.**  $uvby\beta$  indices obtained for HD 205 and comparison stars. The pairs below the star names are the number of points collected for each object in  $uvby$  and  $\beta$ , respectively. The values given by Olsen (1996) are listed in the bottom part.

Object	$V$ (mag)	$b - y$ (mag)	$m_1$ (mag)	$c_1$ (mag)	$\beta$ (mag)
HD 205	8.730	0.231	0.149	0.907	2.753
(905, 4)	14	5	5	13	13
C1 = HD 225273	8.137	0.311	0.157	0.492	2.652
(722, 4)					
C2 = HD 912	8.078	0.343	0.149	0.426	2.620
(436, 4)	4	4	4	8	11
HD 205	8.733	0.220	0.153	0.910	2.757
C1 = HD 225273	8.136	0.317	0.158	0.492	2.650
C2 = HD 912	8.075	0.349	0.144	0.424	2.617

#### 3.2. The variable

To estimate the physical parameters of HD 205, we followed the method described by Rodríguez et al. (2001); the results are summarized in Table 2. HD 205 was not measured by the Hipparcos satellite and, hence, only a photometric  $M_v$  value for the absolute visual luminosity could be determined by use of the relations by Crawford (1979). The derived values (see Table 2) indicate that this star is a normal Population I  $\delta$  Sct-type variable with approximately solar metallicity located in the  $\delta$  Sct region as shown in Fig. 1. In fact, HD 205 just lies on the extrapolation of the blue edge of the  $\gamma$  Dor region to higher luminosities. If evolutionary tracks for  $Z = 0.02$  from Claret (1995) are used, the position of the star is close to the overall contraction phase. Assuming it is still in a main sequence stage, a mass of  $2.23(\pm 0.1) M_\odot$  and age of  $0.9(\pm 0.1)$  Gyr are estimated. If the star had already evolved off the main sequence, values of  $2.08 M_\odot$  and 1.1 Gyr are found.

Other routines for calibration were additionally used to check the values determined above and very good agreement was found. The model-atmosphere grids of Moon & Dworetzky (1985) led to effective temperature and surface gravity values of  $T_e = 7220$  K and  $\log g = 3.50$ . The luminosity calibrations of Domingo & Figueres (1999) resulted in  $M_v = 1^m15$  which also compares very well with  $1^m03$  determined from the Crawford's (1979) relations. Finally, the above derived values for mass, radius and surface gravity were also checked using the biparametric calibrations of Ribas et al. (1997). In this case, values of  $M = 2.06 M_\odot$ ,  $R = 3.22 R_\odot$  and  $\log g = 3.73$  were found.

### 4. Frequency analysis

The frequency analysis was carried out using the method described by Rodríguez et al. (1998) where single-frequency and multiple-frequency techniques are combined using both Fourier and multiple least squares algorithms. Experience with previous works showed that this package yields identical conclusions as the PERIOD98 (Sperl 1998) program.

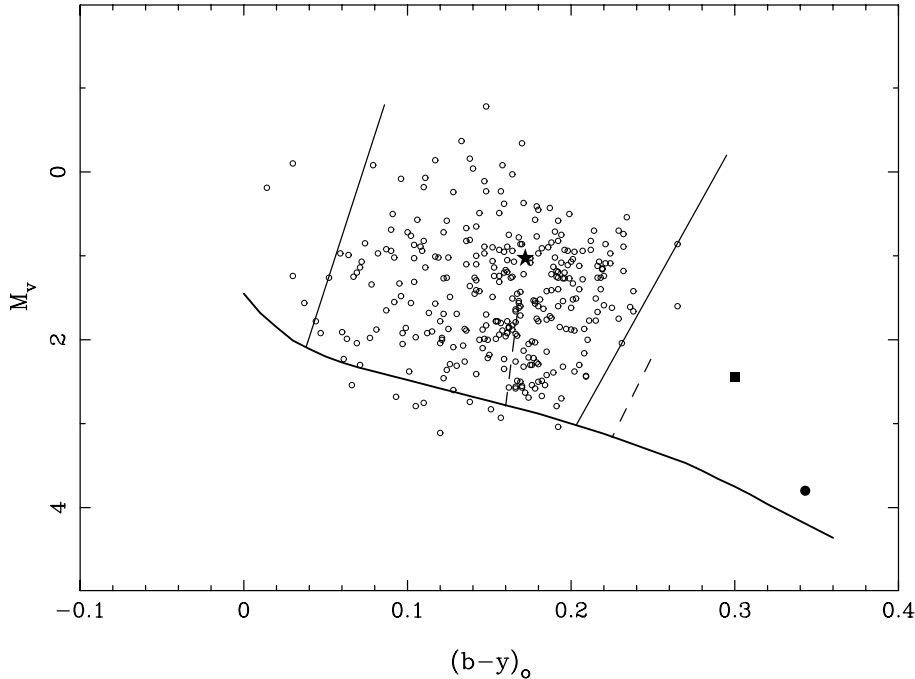


**Fig. 1.** Locations of HD 205 (star), C1 = HD 225273 (square) and C2 = HD 912 (circle) in the H-R diagram together with the  $\delta$  Sct-type pulsators from Rodríguez & Breger (2001). The edges of the observational  $\gamma$  Dor region (dashed lines), from Handler (1999), are also shown.

**Table 2.** Reddening and derived physical parameters for HD 205. Masses and ages corresponding to two different evolutionary stages (main and post-main sequence) are listed.

Parameter	Value	Parameter	Value
$E(b-y)$	$0^m059 \pm 0.01$	$M_{\text{bol}}$	$1^m04 \pm 0.3$
$(b-y)_0$	$0^m172 \pm 0.01$	$D.M.$	$7^m45 \pm 0.3$
$m_0$	$0^m168 \pm 0.01$	$\log L/L_{\odot}$	$1.48 \pm 0.12$
$c_0$	$0^m895 \pm 0.01$	$T_e$ (K)	$7190 \pm 150$
$\delta m_1$	$0^m018 \pm 0.01$	$\log g$	$3.60 \pm 0.1$
$\delta c_1$	$0^m209 \pm 0.02$	Age (Gyr)	$0.9-1.1 \pm 0.1$
[Me/H]	$-0.11 \pm 0.1$	$M/M_{\odot}$	$2.23-2.08 \pm 0.1$
$M_v$	$1^m03 \pm 0.3$	$R/R_{\odot}$	$3.50 \pm 0.6$

Before analysing the frequency content in the light curves of HD 205, it is important to investigate the existence of possible periodicities in the comparison stars due to binarity or spots. Moreover, because the time distribution of the observations and brightness are very similar for both HD 205 and C2, investigation of the C2-C1 Fourier spectra gives us insight on the noise level and precision expected in our conclusions concerning the variable. This fact is of special importance in the range of low frequencies because here is where the instrumental or atmospheric problems such as bad extinction corrections, slow instrumental drifts or nightly zero-point shifts generally manifest themselves. These effects cause spurious peaks in the low frequency domain and special care must be taken to verify if low-frequency peaks are intrinsic to the target star.

In the present work, no such effects seem to be present. The amplitude spectrum for C2-C1 is shown in Fig. 2 for the  $v$  band

in the range  $0-50 \text{ cd}^{-1}$ . The graph resembles that produced by white noise with similar rms and time distribution. Similar behaviour was found in the other bands. No periodicities with amplitudes larger than about 1 mmag are present. The amplitude spectrum is flat over the whole frequency domain, with a mean noise level of about 0.35 mmag. This mean noise level was calculated following Handler et al. (1996), that is, as the average amplitude in an oversampled (by a factor of 20) amplitude spectrum in the frequency domain  $0-50 \text{ cd}^{-1}$ . Hence, the significance level is 1.4 mmag according to the empirically determined limit by Breger et al. (1993, 1996) (amplitude signal-to-noise ratio  $S/N \geq 4.0$  for a signal to be judged intrinsic), which we adopt for the remainder of this paper. This limit is a more conservative threshold than one would obtain from a strictly statistical treatment, but agrees very well with experience in analyses of this type of observational data sets. Hence, periodicities with amplitudes larger than this limit in the amplitude spectra of HD 205-C1 are neither due to the comparison star nor caused by instrumental or atmospheric problems. Nevertheless, the existence of each peak will be checked in all the four  $uvby$  bands as an additional test, and the relations between the amplitudes in different filters will provide us additional information on its physical cause.

As usual, when  $uvby$  photometry is used to investigate pulsational variability in A-F stars, the two filters  $v$  and  $b$  are the first ones to be analysed because both amplitudes and intensities are largest in these two bands and hence the corresponding amplitude  $S/N$  ratios will be highest. In our case, when the  $v$  filter is analysed, six frequencies are significant in the range between 5 to  $14 \text{ cd}^{-1}$ :  $f_1 = 6.249$ ,  $f_2 = 5.338$ ,  $f_3 = 13.285$ ,  $f_4 = 7.714$ ,  $f_5 = 6.685$  and  $f_6 = 11.155 \text{ cd}^{-1}$ . When  $f_1$  is extracted from the data, three new peaks are evident. When the

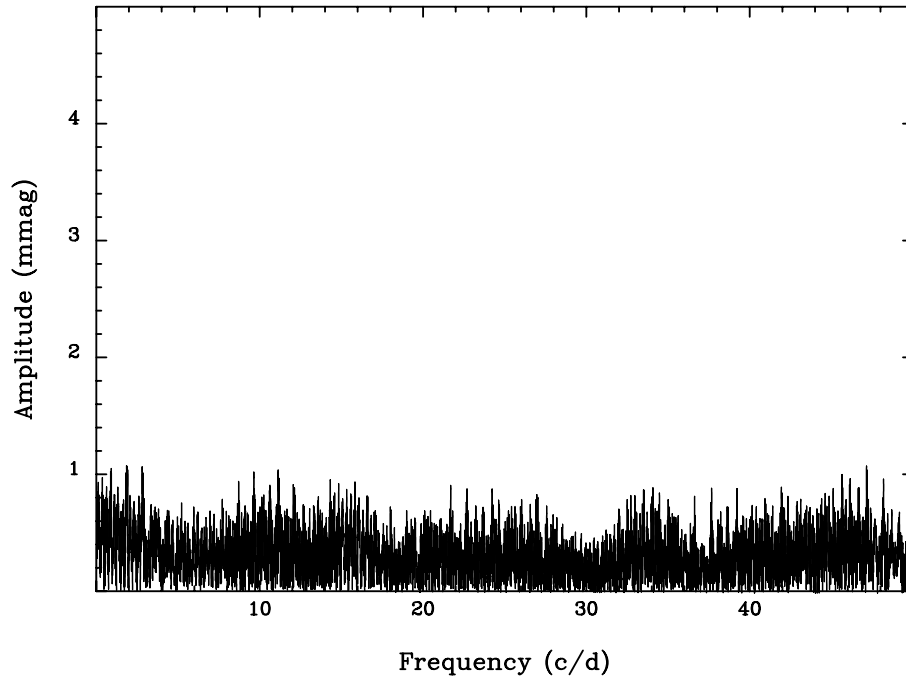


**Fig. 2.** Amplitude spectrum of C2-C1 in the Strömgren  $v$  band.

four frequencies are simultaneously optimized and removed,  $f_5$  and  $f_6$  appear. After prewhitening the six frequencies, no definite peaks can be clearly detected although it is evident that the residuals are too large and more periodicities must remain in the light curves. In fact, the residuals in the region of frequencies lower than about  $15 \text{ cd}^{-1}$  are much higher than in the domain of higher frequencies. The presence of more frequencies in the variable star data is also implied if we consider the amplitude spectrum of C2-C1 (Fig. 2) as a reference.

If the  $b$  filter data are analysed, similar conclusions are obtained and the same set of frequencies is found within  $0.001 \text{ cd}^{-1}$ . In all cases the amplitude  $S/N$  ratios are larger than 4.0 for each of the signals. Similar results were also obtained for the filters  $u$  and  $y$ , but there the  $S/N$  ratio is slightly smaller than 4.0 for  $f_6$  (3.9 and 3.3, respectively). To summarize, we are (except for possible alias problems) confident about the detection of six frequencies.

However, the differences in the  $S/N$  ratios obtained in the four filters due to the different noise levels and amplitudes may cause some uncertainties. For the sake of gaining consistency in the results (set of frequencies and the frequencies themselves) and to obtain a unique solution applicable to all four  $uvby$  filters, we consider the combined  $vby$  “filter” by aligning the  $vby$  data. We can then also investigate the detectability of new peaks. Therefore a weighting scheme will be adopted in the next sections as well.

#### 4.1. Combined $vby$ filter

The combined  $vby$  “filter” was built by merging the observational  $vby$  data following the method described by Rodríguez et al. (2001). Filter  $u$  was not considered because it is the noisiest and it is phase shifted with respect to the other three. In the

**Table 3.** Frequencies, amplitudes and ratios of amplitude signal/noise obtained for the combined  $vby$  filter.

Frequency ( $\text{cd}^{-1}$ )	Amplitude (mmag)	$S/N$
	$\pm 0.41$	
$f_1 = 6.2493$	15.83	14.4
3		
$f_2 = 5.3382$	12.88	11.7
4		
$f_3 = 13.2851$	10.64	8.9
4		
$f_4 = 7.7140$	7.84	7.1
6		
$f_5 = 6.6841$	6.76	6.1
8		
$f_6 = 11.1550$	5.44	4.5
8		

present case, scale factors of 1.163 and 1.414 were used for  $b$  and  $y$  filters, respectively, to transform to  $v$  amplitudes. In each filter, the transformation factor was experimentally calculated with weighting according to the amplitudes obtained for the four main frequencies. Next, the  $vby$  measurements obtained at each instant were averaged with weights according to the precision (that is, the square of the internal error per observation) in each filter. The corresponding weights were 1.0, 1.162 and 0.694 for  $v$ ,  $b$  and  $y$  respectively. With this procedure we also get better precision in the data to analyse. As an example, the rms scatter for C2-C1 and  $vby$  “filter” is of 3.1 mmag as compared to 3.7, 3.4 and 4.1 mmag found for the single filters  $v$ ,  $b$  and  $y$ .

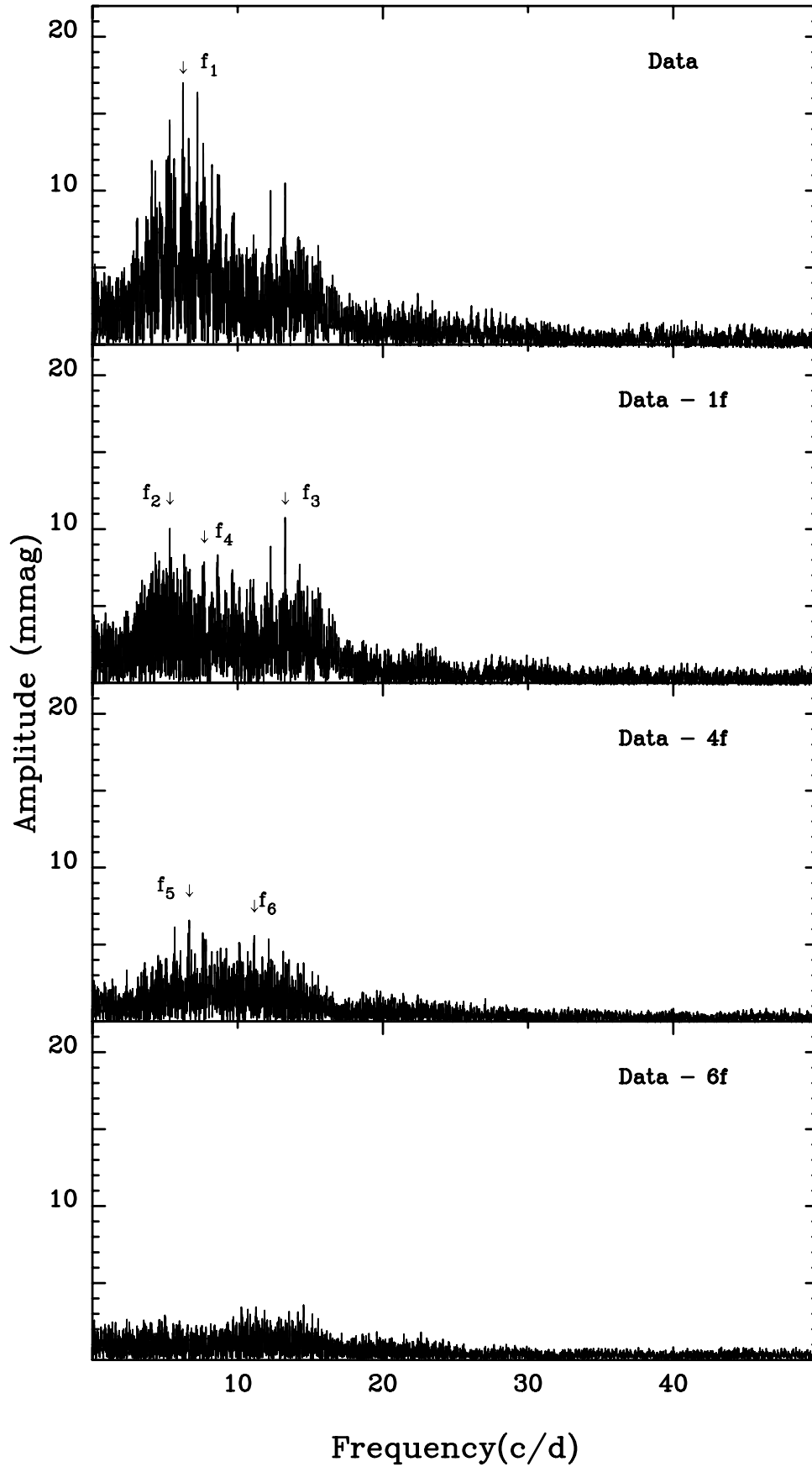


**Fig. 3.** Amplitude spectra of HD 205 in the combined *vby* band corresponding to the “original” data and the results after removing different sets of simultaneously optimized peaks.

**Table 4.** Results from the Fourier analysis applied to the four *u**by* filters. The corresponding signal/noise (*S/N*) ratios are also listed.

Frequency ( $\text{cd}^{-1}$ )	<i>u</i>			<i>v</i>			<i>b</i>			<i>y</i>		
	<i>A</i> (mmag)	$\varphi$ (rad)	<i>S/N</i>									
	$\pm 0.61$			$\pm 0.40$			$\pm 0.36$			$\pm 0.34$		
$f_1 = 6.2493$	12.91	2.693	11.7	15.92	2.452	14.5	13.54	2.476	14.6	11.17	2.440	14.0
		48			25			26			30	
$f_2 = 5.3382$	9.54	4.444	8.7	12.75	4.337	11.6	11.20	4.357	12.0	9.23	4.403	11.5
		59			29			30			34	
$f_3 = 13.2851$	8.42	1.579	7.7	10.54	1.450	8.8	9.20	1.452	8.4	7.54	1.469	7.9
		64			33			34			39	
$f_4 = 7.7140$	5.75	1.789	5.2	7.92	1.565	7.2	6.76	1.591	7.3	5.42	1.597	6.4
		97			46			48			57	
$f_5 = 6.6841$	4.74	3.508	4.3	6.78	3.437	6.2	5.93	3.400	6.4	4.61	3.289	5.8
		115			53			54			65	
$f_6 = 11.1550$	3.72	6.042	3.4	5.64	5.956	4.7	4.52	5.968	4.1	3.85	5.915	4.1
		143			62			69			76	
mean value (mag)	0.7516			0.4258			0.5139			0.5938		
residuals (mmag)	4			2			2			2		
$T_{\text{or}}$ (HJD)	11.0			7.2			6.4			6.0		

The combined *vby* filter data for the variable were analysed leading to a similar set of six frequencies. The results are shown in Fig. 3 and Table 3 with the derived amplitude *S/N* ratios always larger than 4.0. Next, we fixed this set of frequencies and the corresponding fitting for each of the four *u**by* filters was derived. The results are listed in Table 4 with amplitudes, phases and *S/N* ratios. The error bars tabulated in Tables 3 and 4 for frequencies, amplitudes and phases are the formal error bars obtained from the corresponding fits. They are similar to those which we can also obtain using the formulae by Montgomery & O’Donoghue (1999).

However, Fig. 3 suggests that several periodicities with frequencies  $\leq 15 \text{ cd}^{-1}$  still remain in the light curves although it is very difficult to single out the real peaks with the present data. It is also suggested by the large residuals remaining in Table 4. As an example, filter *v* has a rms residual of 7.2 mmag, much higher than the 3.7 mmag which we have for the same filter and C2-C1. This means that several frequencies are still present in the residual light curves. This is confirmed by the fact that the residuals decrease from filters *v* to *b* and *y*. The residuals in filters *v* and *b* can be explained in part as due to better precision of the observations collected in the *b* filter and also because of the smaller amplitudes of the remaining periodicities in this filter. However, the precision of the measurements is worse in the *y* filter. Hence, lower residuals can only be explained by lower amplitudes of the remaining periodicities. On the other hand, in the *u* filter the measurement noise in the residuals dominates over the remaining signals.

An alternative interpretation for the present inadequacy of the multifrequency solution would be that amplitude and/or frequency variations of HD 205 have occurred during the

observations. However, as the time scales typically involved in such phenomena are long compared to the length of our data set, we do not regard this as a reasonable explanation. Figure 4 shows the observed light variations of HD 205 in the *v* filter together with the fit corresponding to the six frequencies. In some parts the agreement with the synthetic curves is not good.

## 4.2. Weighted data

### 4.2.1. Method

For the sake of detecting new intrinsic peaks in the amplitude spectrum of the variable, weights were considered for our combined *vby* data. These weights are based on smoothing the remaining residuals from the solution obtained before. Nevertheless, the assigned weights are independent of the previously found solution for unweighted data. In our case, the weights were assumed point by point individually, according to their intrinsic dispersion as a measure of the quality of the data. However, a problem arises when this dispersion has to determine because a reference line is needed to calculate the deviation of each observational point and, hence, its quality (quality being inverse to the deviation). The simplest case would be to compare the observational points with the synthetic solution previously obtained for unweighted data, as in Fig. 4, but this method is not good because the resulting weights should then depend on the predetermined solution and no new information would be found. A more suitable method consists of deriving nightly reference lines as smoothed lines from the observational data. However, this method has the problem that reliable fits are not easy to determine if pronounced light curves

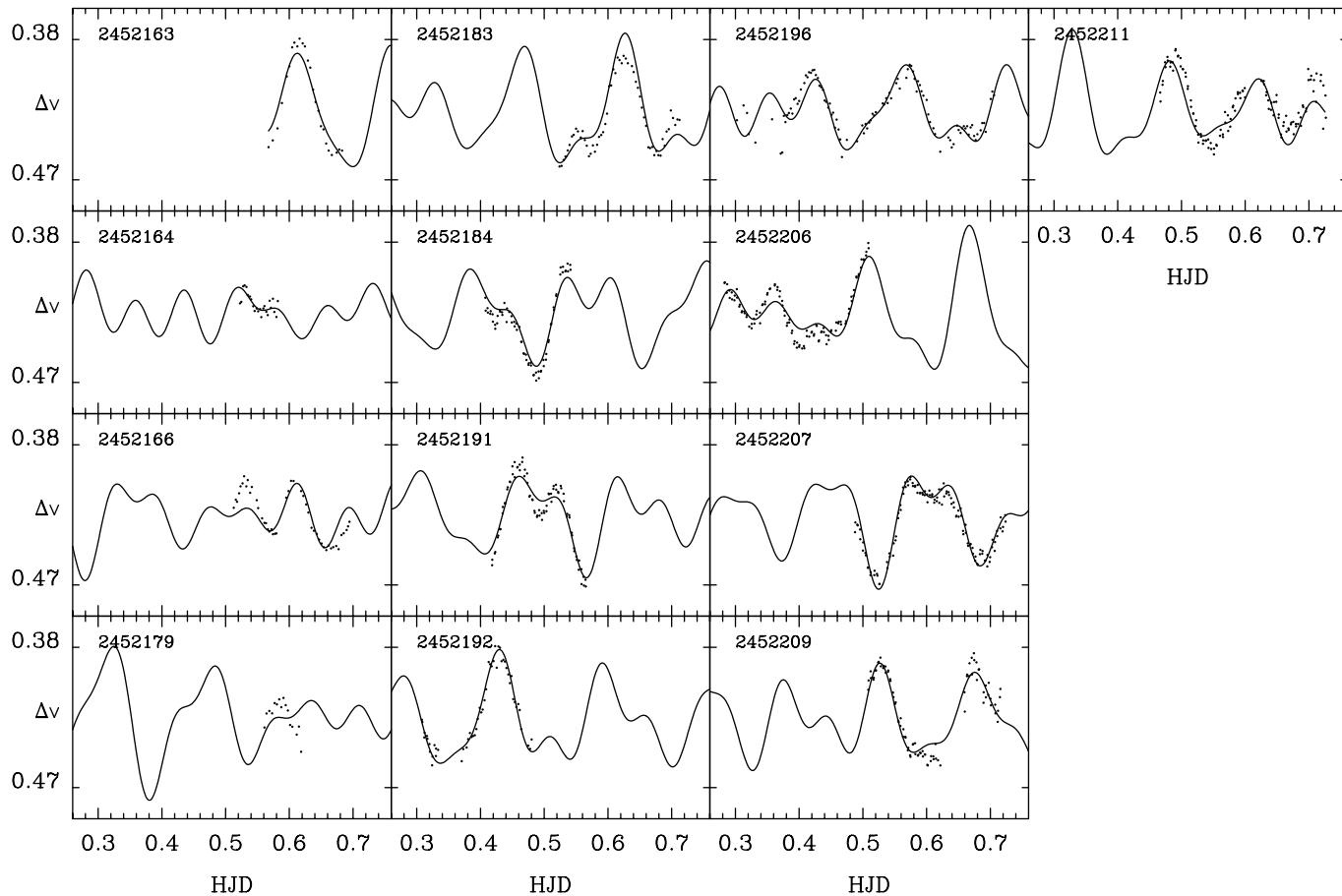


**Fig. 4.** Observed light variations of HD 205 in the  $v$  band together with the Fourier fitting solution of the six frequencies listed in Table 4.

are the subject of study. Only nights with very good and continuous data are suitable for this purpose. This means that a number of nights would be left out of the analysis. Another option would be to derive the dispersion using the comparison stars, because here the differential magnitudes should directly reflect the observing conditions. However, it becomes problematic if no data of the second comparison star have been collected in some nights where the variable was measured.

The most general and suitable method would then consist of using the residuals from a previously known solution, as in Fig. 5, where we present the residuals after removing the set of six frequencies derived before. The corresponding light curves have much lesser variation than the original ones and determining the corresponding mean synthetic lines is much easier. Consequently, smoothing was performed using cubic splines routines, from IMSL Numerical Libraries, over the residuals. Sometimes, when the data are too sparse and simple smoothing by cubic splines did not work, the data were previously averaged using a running Gaussian function with a selected bandwidth. Nevertheless, a few observational points, especially at the beginning of the run corresponding to JD = 2452196, had to be eliminated in the analysis because they were too dispersed to calculate any reliable mean smoothing line. The results can be seen in Fig. 5 where the calculated synthetic lines describe the behaviour of the residuals very well.

Next, deviations of each point  $i$ ,  $\sigma_i$ , are calculated and compared with the mean value  $\sigma$  and the weights  $w_i$  are assigned. In the present work, a value of 2.9 mmag was derived for the mean value  $\sigma$ . Then, weights of  $w_i = 1.0$  are assumed for all points with deviations less than a certain limit; they decrease quadratically as the deviation increases. Experience with previous works showed that  $1.0\sigma$  is a good limit for our calculations, that is, the scheme assumed is  $w_i = 1.0$  for points with  $\sigma_i \leq \sigma$  and  $w_i = (\sigma/\sigma_i)^2$  for  $\sigma_i > \sigma$ .

#### 4.2.2. Results

After weights were assigned to each combined  $vby$  point, a frequency analysis was made on the residuals from the six-frequency solution listed in Table 5. These weighted residuals are shown in the first panel of Fig. 6 where a new peak is present at  $f_7 = 14.56 \text{ cd}^{-1}$ . Because of the weighting, the standard deviation rms of the residuals decreases appreciably. In particular, for the  $vby$  filter, rms decreases from 7.1 mmag (final residuals after extracting the six main frequencies) to 5.9 mmag (the new value of rms after that weights are assigned). This is a 17% improvement, which is however partly (6%) caused by removing a few bad points as mentioned before. The corresponding decrease in each of the individual filters was of 12%, 14%, 17% and 13% for  $u$ ,  $v$ ,  $b$  and  $y$ , respectively.

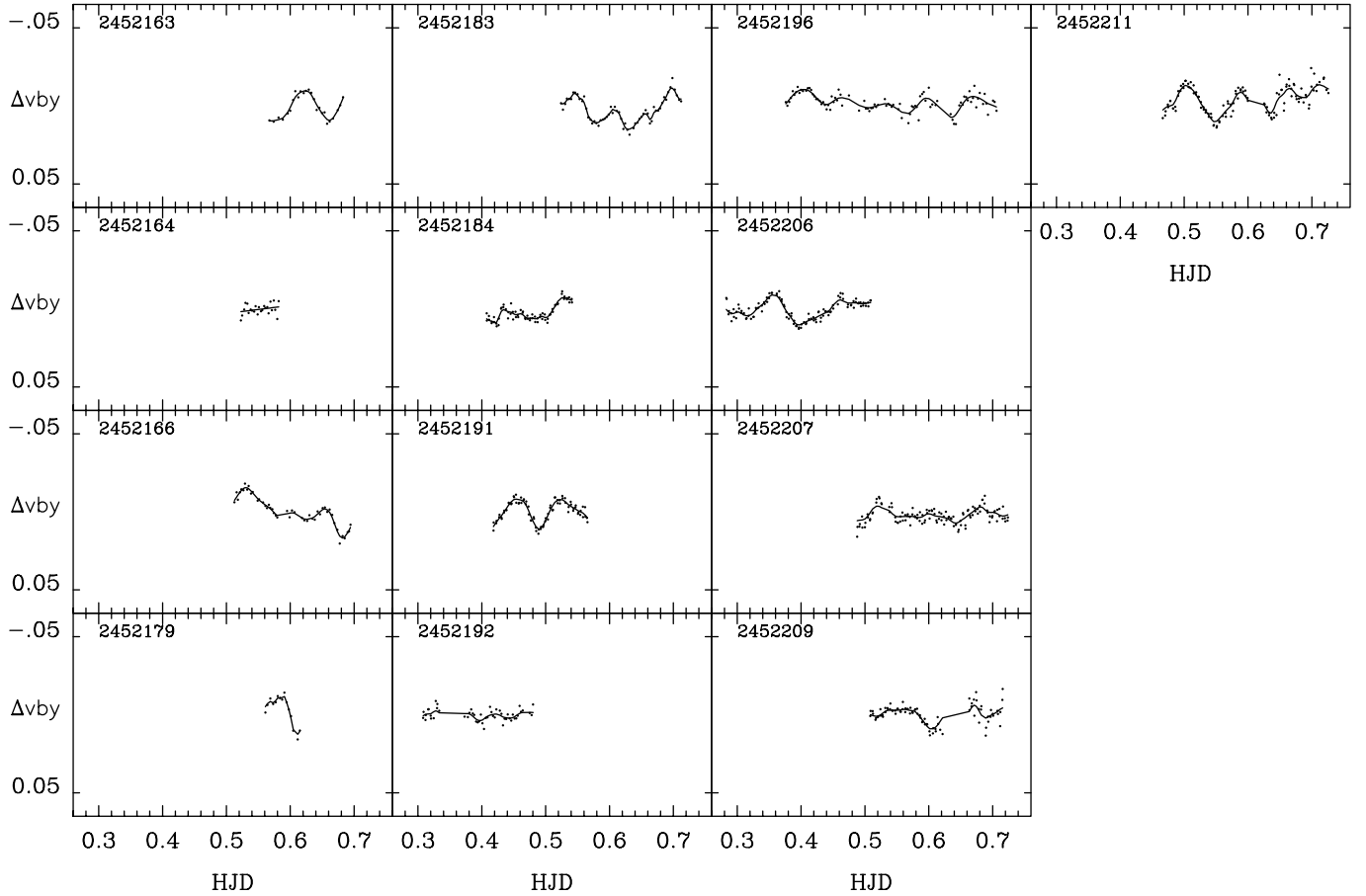


**Fig. 5.** Residuals in the combined *vby* filter after six frequencies together with the corresponding calculated smoothing lines.

When  $f_7$  is removed from the light curves, two new peaks ( $10.27$  and  $5.05$   $\text{cd}^{-1}$ ) can be discerned in the amplitude spectra. The frequencies and amplitudes of the new peaks are listed in Table 5. They all have amplitude  $S/N$  ratios larger than 4.0. The reliability of these new peaks is supported when the solution is applied to each of the four single filters. The results are listed in Table 6 together with the amplitude ratios with respect to the  $v$  filter. These amplitude ratios are of the same order as we can derive for any of the six main frequencies previously found. This suggests that the three new peaks are also pulsational signals.

In the third panel of Fig. 6 the residuals are shown after extracting the three new frequencies. For comparison, the lowest panel contains an amplitude spectrum of white noise corresponding to a dataset with the same time distribution and dispersion ( $\sigma = 2.9$  mmag) as the observations in the combined *vby* filter. It is evident that a number of intrinsic periodicities still remain in the region lower than  $15$   $\text{cd}^{-1}$ . An example would be the peak at  $10.72$   $\text{cd}^{-1}$ , but its reliability is low using only the present dataset. We have therefore demonstrated that weighting can be useful to detect more intrinsic signals. In fact, the frequencies  $f_7$ ,  $f_8$  and  $f_9$  are present at a lower significance level ( $S/N = 3.2$ ,  $2.7$  and  $2.6$ , respectively) before the weighting is introduced in the analysis. Nevertheless, here aliasing is certainly a bigger problem than  $S/N$  in the determination of pulsation frequencies.

**Table 5.** Additional frequencies, amplitudes and signal/noise ratios obtained for the weighted data in the *vby* “filter”.

Frequency ( $\text{cd}^{-1}$ )	Amplitude (mmag)	$S/N$
	$\pm 0.30$	
$f_7 = 14.5564$	3.47	5.3
7		
$f_8 = 10.2738$	3.24	4.7
8		
$f_9 = 5.0499$	3.05	4.2
9		

Pulsation constants  $Q_i$  corresponding to each of the frequencies detected in HD 205 can be calculated using the empirical formula derived by Petersen & Jørgensen (1972). The results are listed in Table 7. As usual in  $\delta$  Sct-type variables, the majority of the frequencies detected correspond to nonradial p-modes of low order. Two regions of preference seem to be present in the ranges about  $5$ – $7$   $\text{cd}^{-1}$  and  $10$ – $14$   $\text{cd}^{-1}$ , but a mode identification for the detected frequencies is obviously premature in the present stage. However, the complex behaviour of its light curves make this variable as a very good candidate to deserve further study through multisite campaigns.

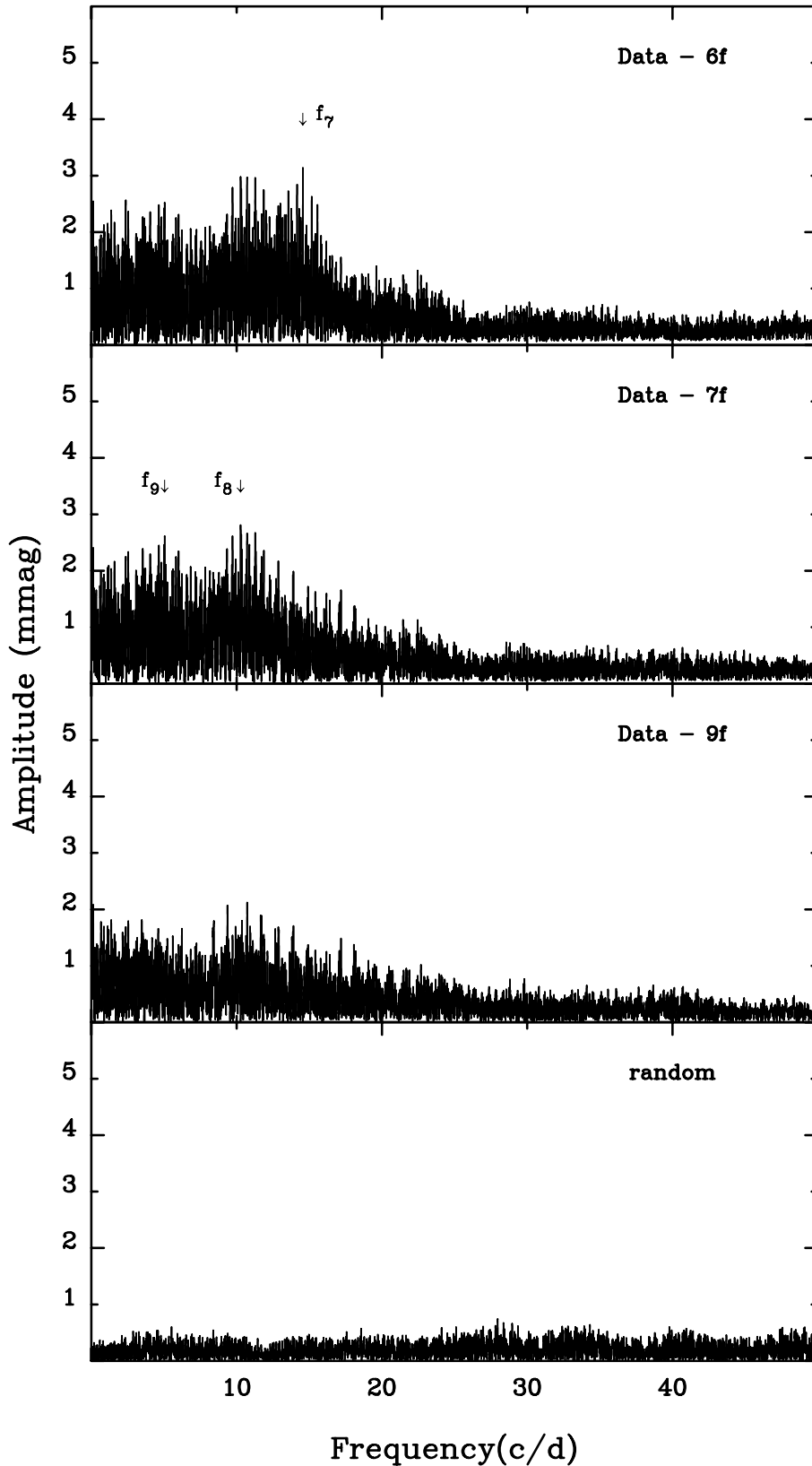


**Fig. 6.** Amplitude spectra of the residuals if weighted data in the combined *vby* band are considered, after than 6 (first panel), 7 (second panel) and 9 (third panel) frequencies are removed. Bottom panel: comparison with an amplitude spectrum of randomly generated residuals.

*Acknowledgements.* This research was supported by the Junta de Andalucía and the Dirección General de Investigación (DGI) under

project AYA2000-1559. This research has made use of the Simbad database, operated at CDS, Strasbourg, France.

**Table 6.** Results for the new frequencies as applied to the four *wby* filters.

Frequency ( $\text{cd}^{-1}$ )	<i>u</i>			<i>v</i>		<i>b</i>			<i>y</i>		
	A (mmag)	<i>S/N</i>	$\Delta v/\Delta u$	A (mmag)	<i>S/N</i>	A (mmag)	<i>S/N</i>	$\Delta v/\Delta b$	A (mmag)	<i>S/N</i>	$\Delta v/\Delta y$
	$\pm 0.48$			$\pm 0.25$		$\pm 0.22$			$\pm 0.23$		
$f_7 = 14.5564$	2.94	4.1	1.12	3.28	5.1	3.01	5.3	1.09	2.63	4.7	1.25
$f_8 = 10.2738$	2.76	3.6	1.20	3.31	4.9	2.73	4.6	1.21	2.33	4.2	1.42
$f_9 = 5.0499$	2.53	3.0	1.23	3.11	4.3	2.63	4.2	1.18	2.10	3.9	1.48
residuals (mmag)	9.3			4.9		4.2			4.5		

**Table 7.** Pulsation constants for the frequencies detected in HD 205.

Freq. ( $\text{cd}^{-1}$ )	Freq. ( $\mu\text{Hz}$ )	$Q(\text{d})$
$f_1 = 6.2493$	72.33	0.032
$f_2 = 5.3382$	61.78	0.038
$f_3 = 13.2851$	153.76	0.015
$f_4 = 7.7140$	89.28	0.026
$f_5 = 6.6841$	77.36	0.030
$f_6 = 11.1550$	129.11	0.018
$f_7 = 14.5564$	168.48	0.014
$f_8 = 10.2738$	118.91	0.020
$f_9 = 5.0499$	58.45	0.040

## References

- Antipin, S. 1997, A&A, 326, L1
- Breger, M., Stich, J., Garrido, R., et al. 1993, A&A, 271, 482
- Breger, M., Handler, G., Serkowsch, E., et al. 1996, A&A, 309, 197
- Claret, A. 1995, A&AS, 109, 441
- Crawford, D. L. 1975, AJ, 80, 955
- Crawford, D. L. 1979, AJ, 84, 1858
- Domingo, A., & Figueras, F. 1999, A&A, 343, 446
- ESA 1997, The Hipparcos and Tycho Catalogues, ESA SP-1200
- Handler, G. 1999, MNRAS, 309, L19
- Handler, G., Breger, M., Sullivan, D. J., et al. 1996, A&A, 307, 529
- Hauck, B., & Mermilliod, M. 1998, A&AS, 129, 431
- Montgomery, M. H., & O'Donoghue, D. 1999, Delta Scuti Star Newsletter, 13, 28
- Moon, T. T., & Dworetzky, M. M. 1985, MNRAS, 217, 305
- Nielsen, R. F. 1983, Inst. Theor. Astrophys. Oslo Report No. 59, ed. O. Hauge, 141
- Olsen, E. H. 1983, A&AS, 54, 55
- Olsen, E. H. 1996, private communication
- Perry, C. L., & Johnston, L. 1982, ApJS, 50, 451
- Petersen, J. O., & Jørgensen, H. E. 1972, A&A, 17, 367
- Ribas, I., Jordi, C., Torra, J., & Giménez, A. 1997, A&A, 327, 207
- Rodríguez, E., & Breger, M. 2001, A&A, 366, 178
- Rodríguez, E., González-Bedolla, S. F., Rolland, A., et al. 1997, A&A, 324, 959
- Rodríguez, E., Rolland, A., López-González, M. J., & Costa, V. 1998, A&A, 338, 905
- Rodríguez, E., López-González, M. J., Rolland, A., Costa, V., & González-Bedolla, S. F. 2001, A&A, 376, 489
- Simbad 2002, Simbad Database, CDS, Strasbourg, France
- Sperl, M. 1998, Comm. Asteroseismology, 111, 1